



Monitoring protein crystallization via dynamic light scattering and in-situ diffraction in microfluidic devices

Katharina Foelsch

University of Osnabrueck, Germany

Supervisor: Michael Heymann, CFEL

08 September 2015

Abstract

Solving protein structures at atomic resolution via x-ray crystallography is essential in the medical field especially in drug development. To expand methodical diversity and thereby the quality of solved structures microfluidic devices were developed creating more possibilities in combination of different techniques of crystallography. However, here we manufactured PDMS and x-ray transparent microfluidic chips and used these for x-ray crystallography of a medical relevant protein, called thioredoxin and for DLS measurements to monitor protein crystal nucleation. Furthermore the *in meso* or LCP crystallization technique was first combined with PDMS chips for applying it in membrane protein x-ray crystallography in the future, which has been quite challenging so far.

Table of Content

Introduction and Theory2

Methods.....5

 Chip fabrication.....5

Wafer fabrication.....5

PDMS chips.....6

In situ chips.....6

Dynamic Light Scattering (DLS)7

Crystallography8

Results9

Acknowledgement.....13

References13

 Figures.....14

Introduction and Theory

The structure of a protein can be resolved by x-ray crystallography at atomic resolution. In this technique a crystal of the protein of interest is irradiated by x-ray radiation (Figure 1, A). The diffraction pattern is a result of radiation that is diffracted from protein and the crystal lattice. The outer ranges of the pattern depict higher resolutions (Figure 1, B). An x-ray beam is emitted from an x-ray tube (copper anode for example) and radiation comes from accelerated circulating electrons in the synchrotron. Data is collected in different modes (different angles) and the number of frames as well as exposure time need to be adjusted to the crystal quality and the type of crystallography. After data collection the electron density has to be calculated and the protein sequence is fitted into the resulting electron density map (model building) to fully determine the structure of the protein (Rupp, 2009).

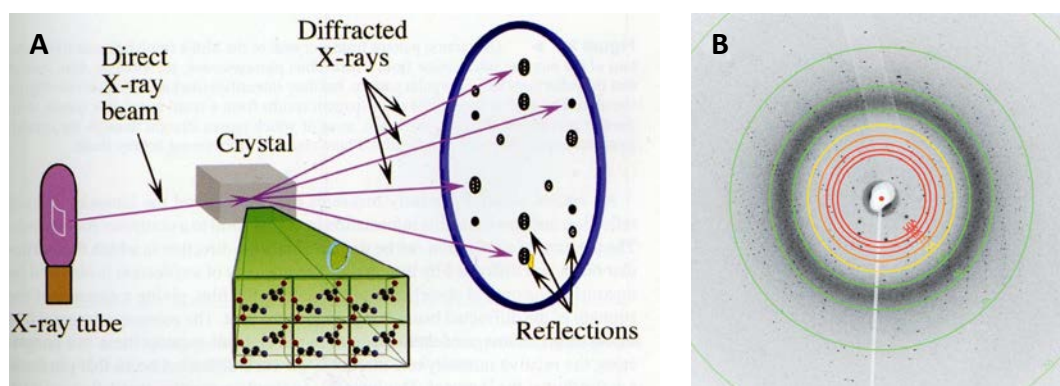


Figure 1: X-ray diffraction. A) Electrons from the x-ray tube hit the crystal that is positioned directly in the beam. The molecules in the crystals are ideally strictly ordered and scatter the x-rays that reach the detector. A diffraction pattern of the reflections is collected. An example of a diffraction pattern is depicted in B. Higher resolutions are given in the outer ranges.

For structure determination by x-ray irradiation a crystal of the protein of interest has to be grown and must be of high purity for satisfying results. There is plenty of different methods that can be made use of and any more conditions, which have to be worked out and optimized to grow a crystal.

Traditionally a data set is obtained from one crystal that has been cryocooled. It has to be long term stable to survive high radiation data collection at its best during the exposure. In contrast to traditional crystallography another approach was developed, called serial crystallography. Here data is collected from non-cryoprotected crystals. Since radiation damage at room temperature is more pronounced the dose is spread over multiple ideally identical crystals. The crystals can be smaller and the conditions do not need to be optimized for freezing. To achieve a high amount of identical crystals, microfluidic devices are well suited as they can prepare and process nanoliter volumes at high-throughput (Guha et al., 2012).

There are many different procedures to grow crystals of a protein. Therefore the protein has to be processed under certain circumstances in high concentrations. The process consists of increasing the supersaturating of the protein in a solution with the optimal precipitant. Most common crystallization methods are vapor diffusion, microbatch, dialysis and free interface diffusion. The procedure of serial crystallography in this work is based on vapor diffusion (Rupp, 2009).

One droplet contains the protein and precipitant, the reservoir is composed of higher concentrated precipitant in buffer. The supersaturating increases (Figure 2, A) as water molecules diffuse to the reservoir until a crystal structure is nucleated. As soon as this moment is reached the supersaturating should be reduced so the crystal can grow, otherwise the protein would completely precipitate (precipitation zone in Figure 2, B).

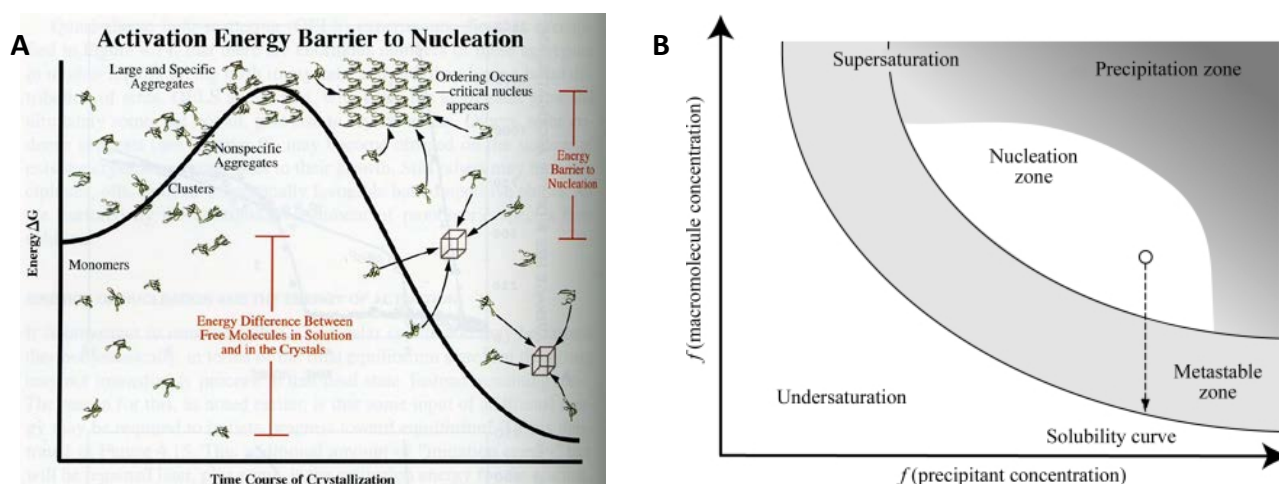


Figure 2: Crystallization. To form a crystal an energy barrier needs to be overcome. The energy barrier to nucleation is shown in A). After enough molecules aggregated to a small nucleus and the energy barrier is passed the energy falls and the crystal grows if the crystallization conditions are optimal. B) By means of different crystallization methods the protein-precipitant solution can be brought from undersaturated to supersaturated state. When the solution reaches the nucleation zone under ideal conditions, the protein molecules aggregate, the concentration of free molecules then falls. In the metastable zone crystals can grow.

One aim of this work was the elaboration of a method to observe nucleation events during crystallization. The dynamic light scattering method is already well suited for this. Here we further elaborated the method in combination with the PDMS and the *in situ* chips. Dynamic light scattering (DLS) is a method to record fluctuation of intensity that is produced by small particles in a solution, which scatter light in all directions. This technique is based on the Brownian motion of the observed particles and depends also on integration time. Through an auto-correlation function the diffusion rate, which is related to size and shape of the particles is determined (Arzenšek, 2010; Santos and Castanho, 1996). Thereby it is obvious that a process of change in molecule size (aggregation) can be analyzed by means of DLS measurements, such as the formation of crystals in particular (Garcia-Caballero et al., 2011; Wilson, 1990). Particles of different sizes can

be distinguished. Recent elaborations and developments were published and are used as foundation for the experiments in this work (Oberthür, 2011; Yu et al., 2012).

Another aim was the production of chips with high signal-to-noise ratio potential for x-ray crystallography of thioredoxin (page 8, Methods, Crystallography). In the last decade microfluidic devices for serial crystallography have been developed. Many crystals are fragile and susceptible to damage caused by light, temperature or other external influences. Thus it makes sense to use a microfluidic device in which the crystallization and the x-ray measurements can be performed (in one) to avoid additional transfers (Guha et al., 2012). Poly(dimethylsiloxane) (PDMS) chips and x-ray transparent chips were produced in this work (Heymann et al., 2014). The chips contain wells, which are connected via channels. The basic idea was the cultivation of one single crystal per well. In Figure 3 a crystal-loaded chip is mounted in the x-ray diffraction setup. The chip is rotatable to vary the viewing angles.

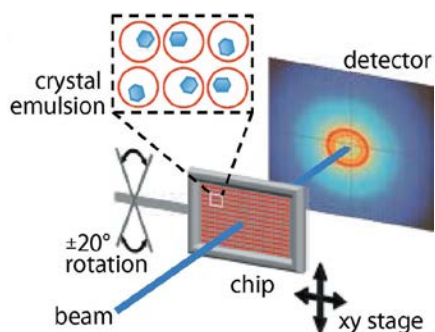


Figure 3: *In situ* serial crystallography. The x-ray beam hits the chip from one well (with crystal) to the next by moving the chip in the xy plane (xy stage). The chip can be rotated by a certain degree of angle. Ideally single crystals grew in each well of the microchip. The diffraction pattern is collected at the detector.

A smaller part of the work was the elaboration of the *in meso* or lipid cubic phase (LCP) technology combined with serial *in chip* crystallography (Caffrey and Cherezov, 2009) with the chip made during this work. Thereby the *in situ* chip technology could be adopted for membrane proteins that can be crystallized by the LCP method. This method is used more and more for crystallization of medical relevant membrane proteins (Caffrey, 2015).

Methods

Chip fabrication

With the software AutoCAD® (from AUTODESK) geometric masks are designed. These are processed to photomasks, which are used to generate a wafer master by photochemistry. This wafer contains the pattern for the chip that consists of channels and wells that match crystals in size. The minimal and maximal size of the mask and chip is limited in flow rates (depending on pressure) and quality of the chosen material. The main procedure is explained in Figure 4. The basic principles for the wafer production and chip manufacturing are explained in the following sections

Wafer fabrication

A photomask is used to process the silicon wafer (Figure 4, 1) according to the protocol of microchem® for SU-8 2000 or SU-8 3000 (Permanent Epoxy Negative Photoresist). At the beginning the wafer is spin coated with SU-8 photoresist and then baked before UV-exposure (known as soft bake). The spin speed during coating determines the desired film thickness. By exposure to UV-light the coated wafer is processed with the photomask (Figure 4, 2). Another baking-procedure is necessary (post exposure bake) to drive cross-linking of the photoresist (Figure 4, 3). According to the UV-exposure time and energy the height of the chip is achieved, for example 50 μm to 100 μm . Finally the coated wafer is developed (Figure 4, 4/5).

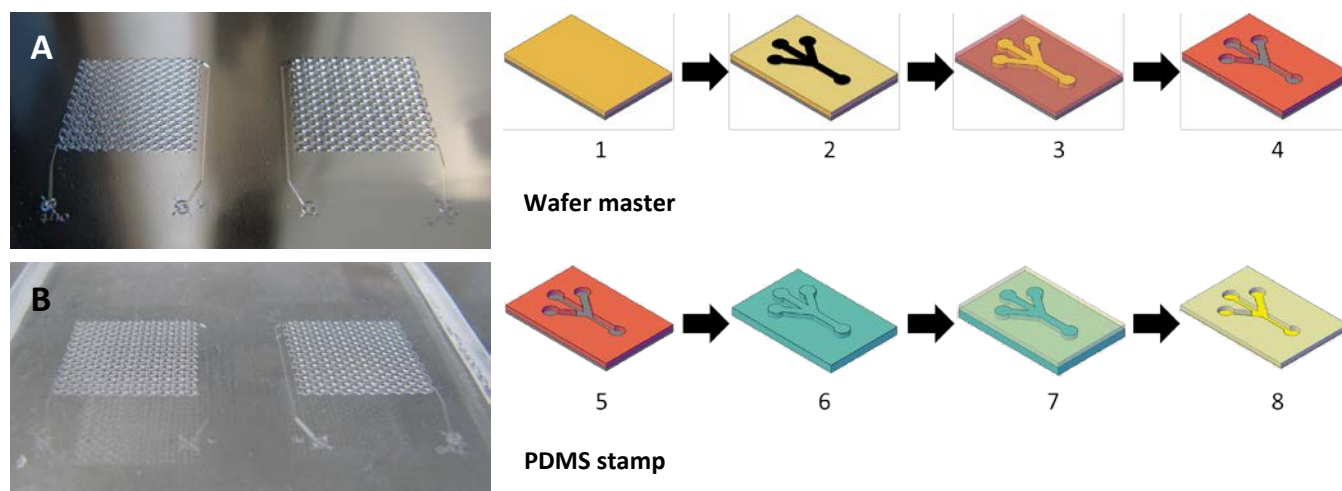


Figure 4: Wafer and chip fabrication. The photoresist is brought onto the silicon wafer blank (1). (2) UV-exposure with photomask after pre-exposure bake (soft bake). After post-exposure bake photoresist is cross-linked (3). Finally the SU-8 master is developed (4/5). Final Wafer master is shown in A. The finished wafer is used as mold for PDMS imprints. According to the wafer production the PDMS cast is used as stamp or again as mold for filling material imprints. The stamp form is shown in 6) and in B. (7) The stamp is poured over with filling material. This stamp is immediately covered with Kapton foil and weight down for an hour. (8) Final Kapton foil with the chip filling material.

PDMS chips

Poly(dimethylsiloxane) (PDMS) is used as material for the molds that form the channels and wells that can be filled with protein mixtures or other reagents. PDMS (184 Silicone elastomer, base and curing agent from Sylgard®) is mixed in a 1:10 ratio of curing agent to base and poured over the master to create an imprint (inverse to Figure 4, step 6). After one hour of baking at 65°C the PDMS layer is cured. The PDMS layer can be peeled off of the wafer and is cleaned or surface activated by means of an oxygen plasma cleaner (ZEPTO from Diener electronic®, plasma-surface-technology) for 30 seconds. A microscope slide (75x50mm, ~1mm thick) is activated the same way and both parts are brought together directly after the activation process. By this procedure channels and wells are formed between PDMS and glass slide. These are coated with Cytop CTL-809M in CTsolv.100E (1:20) (Bellex International). Finally the chips are baked for another hour on a heating plate at 200°C (Folch, 2013; Heymann et al., 2014).

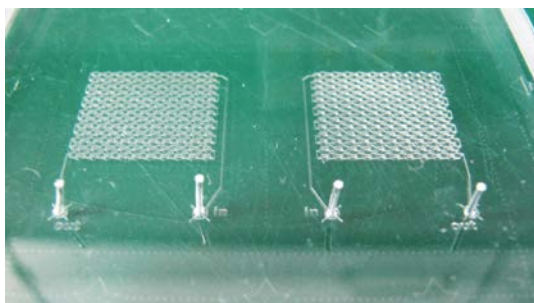


Figure 5: PDMS chip. This picture shows an example of a PDMS chip without valves. This chip has a height of 100 μm , one input and one output for loading. The PDMS layer is connected to the micro glass slide. This is made by use of oxygen plasma activation of the two connected surfaces for 30 seconds in the plasma cleaner. The out- and inputs are pricked out before activation procedure and have a width of 750 μm .

In situ chips

For the production of an x-ray transparent in-situ chip, a PDMS stamp is created first. For this, a master is poured over with a 1:10 mixture of curing agent and base (Figure 4, step 5-6). After 1 h of baking the cured PDMS stamp is peeled off (Figure 4, 6). In step 7 the PDMS stamp is casted with mixture of chip filling material, adopted from Michael Heymann (Heymann et al., 2014). An 8 μm thin Kapton foil (American durafilm®) is placed and pressed to the PDMS stamp. The sandwich of stamp and foil needs to be weight down. Then the Kapton foil can be peeled off. A second layer of foil is brought onto the other. Basically both Kapton foils are activated in oxygen plasma. Both are incubated in different silane, see also silane coupling chemistry adopted from Tang and Lee (Tang and Lee, 2010). These silanes are strongly (1%) diluted in water. Aminopropyltrimethoxysilane and the counterpart glycidoxypyltrimethoxysilane (APS, 97%; GPS, 98%; both from Sigma Aldrich) are strongly diluted (1%) in water for incubation (2 min) of foils. Bringing the both foils into contact the silanes build an epoxy-like bond. The chip is coated from the inside with Cytop CTL-107 EA in CTsolv.100E (1:40) (Bellex International). Completed chips loaded with protein in a crystalline structure can be mounted into appropriate holder to directly collect data.

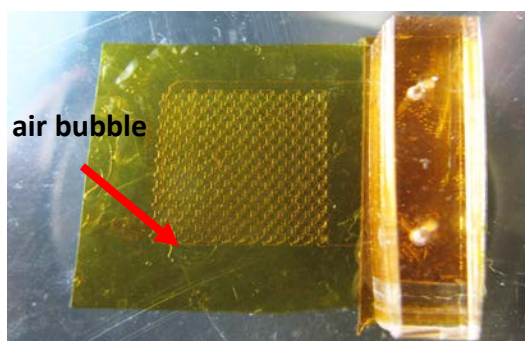


Figure 6: Final x-ray transparent chip. This picture shows a completely finished x-ray transparent chip. The in- and output are extended with a piece of PDMS where the corresponding sections are punched out. The red arrow shows an air bubble between the foils. The air bubble-free manufacturing of the chips is quite challenging. Nevertheless the chip can be used for a few experiments, when the wells can still be loaded.

Dynamic Light Scattering (DLS)

Dynamic light scattering was the chosen method to investigate the nucleation process of different proteins. The use of DLS to observation of protein crystal nucleation was introduced by Garcia-Caballero and colleagues (Garcia-Caballero et al., 2011). The used instrument in this work is named SpectroLight™600 and was produced by *Xtal concepts GmbH*. Settings were varyingly adjusted corresponding to the studied protein approaches and the measurement times. The laser and detector optics both have to be focused in the sample drop at a crossing point. By the autocorrelation function and the Stokes-Einstein equation the hydrodynamic radius of the molecules in the sample volume can be determined. Proteins randomly scatter photons in all directions, which are detected (Santos and Castanho, 1996). The resulting interference fluctuations deliver the needed information for calculations.

Particular details to the instrument are given by the manufacturer (SpectroLight™600 flyer by *xtal concepts*, downloaded on 02.09.2015). Further details are given in following references (Karsten Dierks, 2008; Oberthuer et al., 2012). For basic studies in the beginning we used thaumatin as model protein, which comes from *Thaumatococcus daniellii* (Sigma Aldrich®) and was prepared by Robin Schubert (University of Hamburg).

Protocol thaumatin:

- Protein buffer: 50 mM BisTris pH6.5
 - Protein concentration: 34 mg/ml
 - Precipitant: 0.5 M sodium tartrate
- Precipitant and protein solution was mixed 1 to 1

Crystallography

Protein solution is mixed with the selected precipitant buffer immediately before loading the mixture into the pre-coated chip. Lysozyme from chicken egg white (from Fluka analytical) is used as model system for X-ray experiments in PETRA III beamtime and for DLS measurements. It is mixed with different precipitant approaches that are useful in the corresponding experiments (regulating growth rate of crystals). Standard protein concentration was 50mg/ml, precipitant ingredients were: 0.5-1M sodium chloride, 0.05-0.1M sodium acetate buffer (pH4.5) and 15-30% PEG400.

Protocol lysozyme:

- Protein buffer: 50 mM sodium acetate pH4.6
 - Protein concentration: 50 mg/ml
 - Precipitant: 1 M sodium chloride, 10% PEG5000MME, 100 mM sodium acetate pH4.6
- Precipitant and protein solution was mixed 1 to 1

In this work thioredoxin (Trx, prepared by Svetlana Kapis/University of Hamburg) is the protein of interest and is also mixed with different precipitants to figure out which approach works best with the *in chip* serial crystallography, including the X-ray data collection in the end. Bacteriorhodopsin (bR) is an integral membrane protein produced by extremophile halobacteria and used to investigate the compatibility of the *in meso* or LCP technology with the *in chip* serial crystallography. bR was kindly provided by Jörg Labahn (CSSB).

After loading the chip with one of the protein-precipitant mixtures the chips have to be kept in a wet environment (humidity chamber, sealed by parafilm), otherwise they would dry out through evaporation (PDMS and Kapton foil are both permeable for water vapor). The crystals or crystal nuclei could be damaged or deformed by dehydration.

For x-ray data collection in PETRA III and DLS measurements the chip with grown crystals is mounted onto specially produced holders (by means of a 3D printer).

Petra III p14 setup:

- Beam focus: $5 \times 5 \mu\text{m}^2$
- Flux at 12 keV (ph/s): 5×10^{12}
- Detector: PILATUS 6M, 25 Hz

Results

For x-ray crystallography of thioredoxin a bunch of x-ray transparent chips was loaded with different protein precipitant mixtures provided by Svetlana Kapis. Crystals grew in more than a half of the loaded chips. These were then analyzed in PETRA III at the p14 x-ray diffraction setup. The chips were mounted onto a holder that was printed with a 3D printer. This holder can be rotated for an optimal recording angle. After data collection three of the chips were crosscut to examine the chip quality. Chip quality means the thickness of filling material between the two Kapton foils as it is not completely transparent for x-ray radiation. By making cross-sections of the chips it becomes clear that the filling material layer has a varying height, even within one well (Figure 7, A and B). Pictures A and B show two wells of the same chip and crosscut. The well in A has a constant height which is important for comparability. The filling material of the well in B has varying height which is problematic for comparable and reliable data. Picture C shows a chip of high quality. The filling material in the well is very thin ($\sim 3 \mu\text{m}$) compared to the one in A. In picture A it has the same height like the well itself ($\sim 50 \mu\text{m}$).

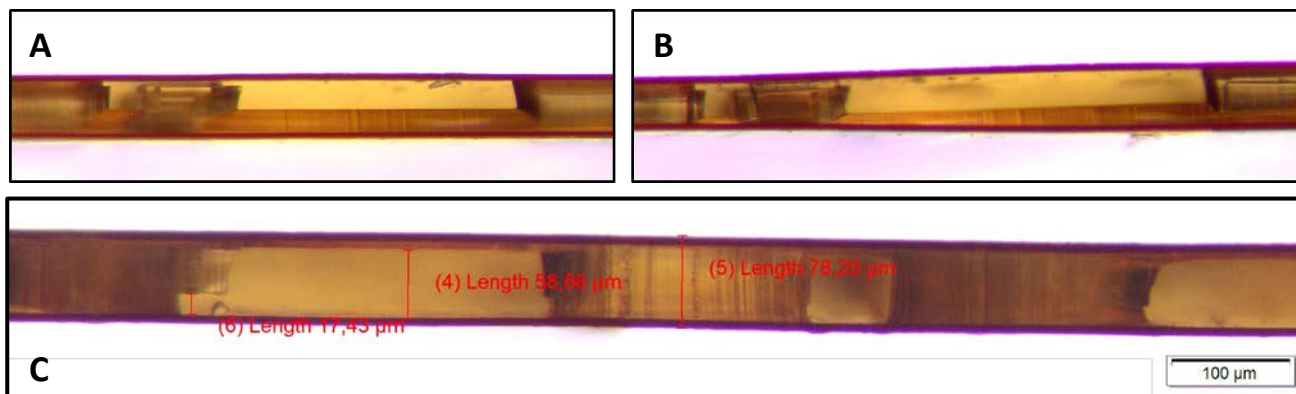


Figure 7: Chip cross sections. After PETRA III beamtime and data collection for thioredoxin, three chips were crosscut to assess the chip quality. After data evaluation it can be seen how chip matches data quality. Pictures A and B show two different wells in the same chip. The filling material has a different height and thereby different signal-to-noise qualities. C shows how a chip of good quality should look like. The filling material layer is thin (about 3-3.5 μm).

The thinner the filling material the better is the signal-to-noise ratio. For improvement of a constant thin filling material the corresponding production step should be modified. The critical point is the step 7 to 8 (Figure 4) where the Kapton foil is pressed onto the PDMS stamp covered with filling material. The weights for the pressing process could be increased and it should be automated. For the chip production the foil was manually pressed onto the stamp and then weight down with several weight bodies. An automated press would distribute the weight in a uniform way. Also the filling material can be modified so that it is more fluid and easier to be driven away from stamp by the foil. Without any improvement the signal-to-noise ratio will be further on low and irregular in many chips, which leads to poor resolution.

Aim of this project (cooperation with Svetlana Kapis) is the visualization of conformational changes in thioredoxin by solving crystal structures of various reaction intermediates at different temperatures. Furthermore the investigation of UV-dose dependent S-S-bond cleavage via pump and probe experiments with the UV-laser. Solving thioredoxin that way is highly interesting as this protein is a promising drug target candidate. It is involved in causing diseases of the lymphatic system (Yousef, 2014).

To investigate the nucleation of protein crystals dynamic light scattering (DLS) measurements were performed at the SpectroLight™600. For experiments the proteins thaumatin, lysozyme and thioredoxin were used. PDMS chips and x-ray transparent chips were loaded and monitored. Recording time for one measurement were 30 second every 5 minutes. For longer observations the interval time was one measurement every 20 minutes. For the instrument a special holders for both types of chips were printed with the 3D printer. The thinner the chip the harder it is to find the right focus within one well for long term recording. Therefore the chips were produced with a well height of 100 μm . DLS measurements were first investigated for PDMS chips loaded with lysozyme to find out the optimal settings for the following experiments with thioredoxin. The measurement is only possible as long as the well is filled with solution, so the limitation is given by evaporation during the crystallization process. Furthermore the crystallization process should not occur too fast as the recording takes some time, especially the individual adjustment for each chip as they are not normed. Figure 8 gives the results for thioredoxin monitored over 21 hours. Every 20 minutes 30 seconds of measurement were performed (A, B) and a picture of the well was taken (C, four selected examples). As the red constant in A demonstrated there is a slight increase in radius over time, so the ratio between bigger and smaller particles rises. The nucleation should happen between the first 11 hours because after that first small crystals are already visible. After 17 hours the crystals reached their maximum in size. The size does not change after that in a significant way. That means, the chip could be used for x-ray structure analysis at this time point. In the picture after 21 hours it the well is half full of air and the measurement stopped after this time because the laser has to be focused in liquid solution for data collection. The pictures from 17 to 21 hours demonstrate the advancing evaporation in the chip. The used PDMS chip was not kept in a closed wet chamber so the evaporation could not be prevented.

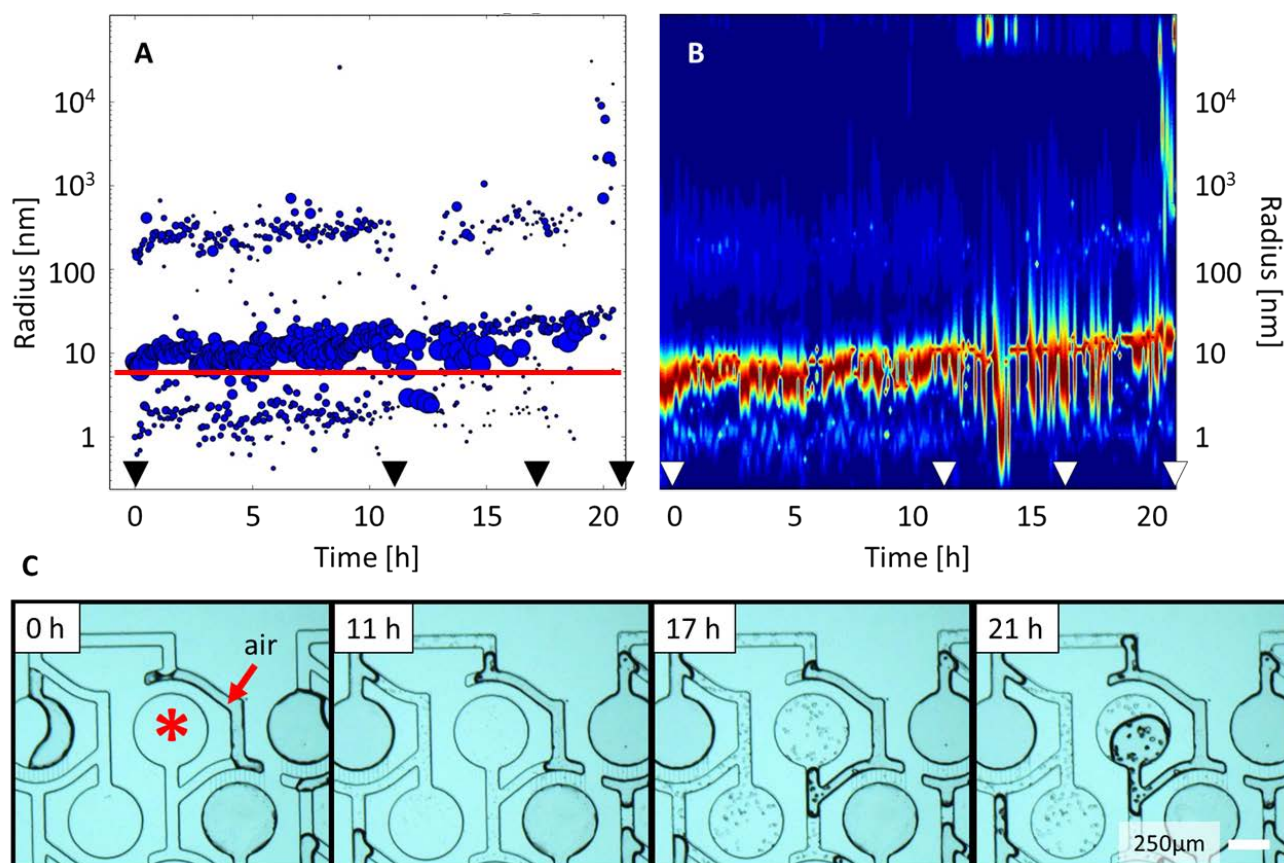


Figure 8: DLS Results for thioredoxin. A) Radius is changing over 21 hours. The size distribution in the measured volume changes as the red constant underlines in A. The sizes of circles in A represent the quantity of measured particles with the corresponding radius. B is another display option for the radius distribution of particles measured over time. Red color means high amount of scattered photons, blue is very low signal. The triangles indicate the time points chosen for the related pictures in C. Here it was measured in a PDMS chip without valves. The red star points out the focus of the incoming laser, red arrow shows an example for an air bubble in the chip channel. After 11 h very small crystal structures are already visible. After 17 h there is a high amount of fully grown crystals in the well and in the surrounding channels. After 21 h the measurement is stopped because the evaporation is far processed.

However, the main aim here is to monitor the nucleation process, meaning the first period in which the crystals are growing. Radius plot and signal intensity distribution is not easy to interpret as there is too little reference material. Even though the results show that there is a change over time and it is worth to further investigate *in chip* protein crystallization approaches with this method. Long term aim is the possibility of observing the crystallization process and the direct intervention. Especially immediately after nucleation the supersaturation needs to be reduced to keep the solution in the meta-phase so crystals can grow under optimal conditions.

Other than ‘simple’ proteins, membrane proteins need special treatment for crystallization. To implement this *in meso* or the lipid cubic phase (LCP) technology is a good method, although development is still advancing. Here we tried to combine our *in chip* crystallization with the LCP technique. Therefore a PDMS chip was pre-loaded with a dilution of monoolein in methanol (1:5) used as host cubic phase lipid (Sigma Aldrich®). After evaporation of methanol the wells were about one fifth filled with monoolein (Figure 9, A –

red arrow). After pre-loading the chip is completely loaded with bacteriorhodopsin in precipitant. We filled 8 PDMS chips with 8 different protein preparations (collaboration with Jörg Labahn). In Figure 9, B is demonstrated how the chip looks like after bR-loading. The red arrow depicts the phase of bR (pink color). In some wells the distribution of protein phase and lipid phase looks typically. In other wells it looks like there is a third uncharacteristic phase recorded (shown by blue arrow).

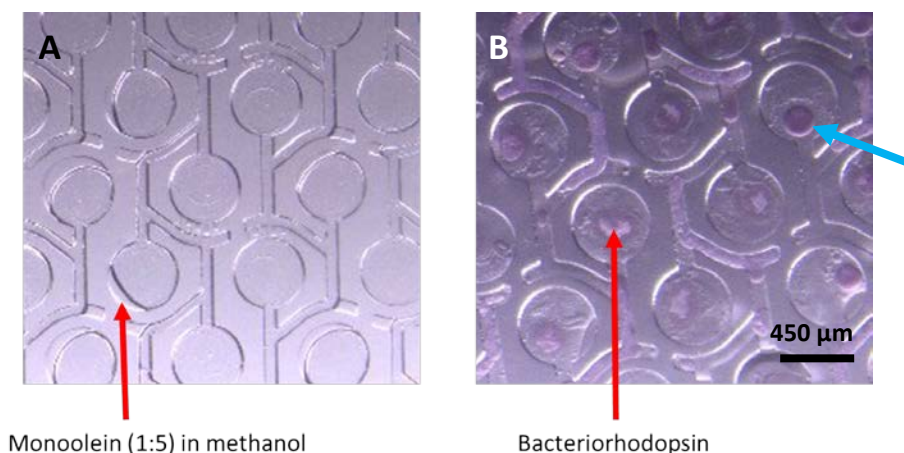


Figure 9: Bacteriorhodopsin crystallization in PDMS chips. PDMS chip is pre-loaded with monoolein 1:5 mixed with methanol. After evaporation of methanol the well is filled with the remaining monoolein (sickle-shaped liquid, red arrow) shown in A. In B the same chip is then loaded with a mixture of bacteriorhodopsin (bR) and precipitant. The red arrow depicts the bR phase (easily visible because of the red color of bR). The bR is well placed in the wells of the chip, but up to now no crystals could be grown. Blue arrow depicts a kind of third phase that is uncharacteristic.

The wet chamber with the chips in it was kept in darkness for potential crystal protection. Even after several days there were no crystals recorded. Furthermore the bR-typical color was changed to brown-greenish, which indicates that the protein is spread and not higher concentrated like it should be during the crystallization process. We assumed that the monoolein loses its functionality by mixing it with methanol or ethanol. Due to several additional experiments it became clear that monoolein does not typically behave after mixing it with alcohol than it does usual. Without any treatment it melts by incubating it at 45°C for a few minutes. When it cools down again it turns back into its hard wax form. When it is in its LCP form mixed with the protein solution it is also waxy, but more like tooth paste (Caffrey, 2015; Liu and Cherezov, 2011). However, as it is once mixed with methanol it cannot get back into its waxy form and maintains to appear oily. To solve this problem and to further work on bR crystallization a new solvent for the monoolein needs to be found. Apart from that another host cubic phase lipid could be tried out. In any case, the lipid has to be fluidly enough for loading and should retain its functionality for successful *in meso* crystallization. Long term aim of this project is the compatibility of *in meso* crystallization and *in chip* x-ray crystallography so structures medical relevant membrane proteins can be solved.

Acknowledgement

I want to thank my supervisor Michael Heymann (CFEL, Hamburg) for guiding me, sharing his projects with me and provide his microfluidic chip equipment that was used. It was a great experience to work in the Chapman group.

Then I want to thank Jörg Labahn (CSSB) for providing bacteriorhodopsin and the collaboration.

The used thaumatin was prepared by Robin Schubert (University of Hamburg) and he strongly contributed to the DLS experiments. Thank you for that!

Finally I want to thank Svetlana Kapis (University of Hamburg) for providing the thioredoxin samples for the DLS measurements and for x-ray crystallography.

References

Arzensek, D. (2010). Dynamic light scattering and application to proteins in solutions (University of Ljubljana).

Caffrey, M. (2015). A comprehensive review of the lipid cubic phase or *in meso* method for crystallizing membrane and soluble proteins and complexes. *Acta Crystallogr. Sect. F Struct. Biol. Commun.* **71**, 3–18.

Caffrey, M., and Cherezov, V. (2009). Crystallizing Membrane Proteins Using Lipidic Mesophases. *Nat. Protoc.* **4**, 706–731.

Folch, A. (2013). Introduction to BioMEMS (Seattle, WA, USA: CRC Press Taylor & Francis Group).

Garcia-Caballero, A., Gavira, J.A., Pineda-Molina, E., Chayen, N.E., Govada, L., Khurshid, S., Saridakis, E., Boudjemline, A., Swann, M.J., Shaw Stewart, P., et al. (2011). Optimization of Protein Crystallization: The OptiCryst Project. *Cryst. Growth Des.* **11**, 2112–2121.

Guha, S., Perry, S.L., Pawate, A.S., and Kenis, P.J.A. (2012). Fabrication of X-ray compatible microfluidic platforms for protein crystallization. *Sens. Actuators B Chem.* **174**, 1–9.

Heymann, M., Ophthalage, A., Wierman, J.L., Akella, S., Szebenyi, D.M.E., Gruner, S.M., and Fraden, S. (2014). Room-temperature serial crystallography using a kinetically optimized microfluidic device for protein crystallization and on-chip X-ray diffraction. *IUCrJ* **1**, 349–360.

Karsten Dierks, A.M. (2008). Dynamic Light Scattering in Protein Crystallization Droplets: Adaptations for Analysis and Optimization of Crystallization Processes. *Cryst. Growth Amp Des.* - CRYST GROWTH DES **8**.

Liu, W., and Cherezov, V. (2011). Crystallization of membrane proteins in lipidic mesophases. *J. Vis. Exp. JoVE*.

Nogly, P., James, D., Wang, D., White, T.A., Zatsepin, N., Shilova, A., Nelson, G., Liu, H., Johansson, L., Heymann, M., et al. (2015). Lipidic cubic phase serial millisecond crystallography using synchrotron radiation. *IUCrJ* **2**, 168–176.

Oberthuer, D., Melero-García, E., Dierks, K., Meyer, A., Betzel, C., Garcia-Caballero, A., and Gavira, J.A. (2012). Monitoring and Scoring Counter-Diffusion Protein Crystallization Experiments in Capillaries by in situ Dynamic Light Scattering. *PLoS ONE* **7**, e33545.

Oberthür, D. (2011). Detailed Analysis of Protein Crystallization and Aggregation Phenomena Applying Dynamic Light Scattering. Dissertation. University of Hamburg.

Rupp, B. (2009). Biomolecular Crystallography: Principles, Practice, and Application to Structural Biology (Garland Science).

Santos, N.C., and Castanho, M.A. (1996). Teaching light scattering spectroscopy: the dimension and shape of tobacco mosaic virus. *Biophys. J.* **71**, 1641–1650.

Tang, L., and Lee, N.Y. (2010). A facile route for irreversible bonding of plastic-PDMS hybrid microdevices at room temperature. *Lab. Chip* **10**, 1274–1280.

Wilson, W.W. (1990). Monitoring crystallization experiments using dynamic light scattering: Assaying and monitoring protein crystallization in solution. *Methods* **1**, 110–117.

Yousef, N. (2014). Structure function analysis of thioredoxin from *Wuchereria bancrofti*, a drug target for human lymphatic filariasis. University of Hamburg.

Yu, Y., Wang, X., Oberthür, D., Meyer, A., Perbandt, M., Duan, L., and Kang, Q. (2012). Design and application of a microfluidic device for protein crystallization using an evaporation-based crystallization technique. *J. Appl. Crystallogr.* **45**, 53–60.

Figures

1 from Rhodes, *Crystallography made crystal clear*, Academic Press (2006)

2 (Nogly et al., 2015)

3 from McPherson, *Crystallization of Biological Macromolecules*, CSHL Press (1999)

4 http://openi.nlm.nih.gov/imgs/512/150/2631111/2631111_d-64-01240-fig1.png (150825)

5 © Michael Heymann